© Universiti Tun Hussein Onn Malaysia Publisher's Office

IJIE

http://penerbit.uthm.edu.my/ojs/index.php/ijie
ISSN : 2229-838X e-ISSN : 2600-7916

The International Journal of Integrated Engineering

Flow Characteristics in Perforated Subsurface Drain of Drainage System Application: Case Study of Gate Fully Open with Longitudinal Slope 1/500

Junaidah Abdullah[1], Mohd Remy Rozainy Mohd Arif Zainol[1,2*], Mohd Fazly Yusof[1], Muhammad Zaki Mohd Kasim[1], Muhamad Nurfasya Alias[1], Khairul Rahmah Ayub[1], Siti Fairuz Juiani[1], Nor Ariza Azizan[1], Syafiq Shaharuddin[1], Muhammad Kashfy Zainalfikry[1], Nor Azazi Zakaria[1], Aminuddin Ab Ghani[1]

[1]River Engineering and Urban Drainage Research Centre,
Universiti Sains Malaysia, 14300 Nibong Tebal, Penang, MALAYSIA

[2]School of Civil Engineering,
Universiti Sains Malaysia, 14300 Nibong Tebal, Penang, MALAYSIA

*Corresponding Author

DOI: https://doi.org/10.30880/ijie.2023.15.02.019
Received 23 February 2023; Accepted 17 May 2023; Available online 31 July 2023

Abstract: Subsurface drainage is part of a sustainable drainage system's components. This component represents the infiltration of stormwater into the subsurface drainage system for flow attenuation purposes. This study examines the flow parameters of subsurface drainage components. The laboratory validation of perforated subsurface drains was conducted at a longitudinal slope gradient of 1/500 with the Gate Fully Open. The manning, n data obtained in these experiments varies with several hydraulic parameters. Therefore, the experimental relationship between the flow characteristics of these subsurface drain components has been investigated. The relationship between flow behavior has been determined. The sub-critical and supercritical, and turbulence flow has occurred in this study.

Keywords: Sustainable urban drainage system, perforated subsurface drain, flow characteristics

1. Introduction

Subsurface drainage systems are installed to drain away subsurface water in order to improve the ground's stability and friction, minimize surface water ponding and waterlogging of soils by decreasing water tables, and increase soil strength by decreasing the soil's moisture content. A significant indicator of the necessity for subsoil drainage is the presence of a highwater table high to damage urban structures and infrastructure. In addition, subsoil drainage is crucial in hilly regions due to the possibility for land instability [1].

Subsurface drainage is accomplished by installing an artificial conduit or flow path underneath the water table such that the conduit's hydraulic head is less than that of the soil to be drained. Common subsoil drain types (Fig. 1) include the basic system, geotextile filter, pipe drain, pipe drain with capping to exclude surface water, geotextile around the pipe, geocomposite drain in a narrow trench, geocomposite drain in a shallow trench, and soil filter layer to prevent geotextile clogging [1].

The use of perforated pipes reduces subgrade moisture, which is crucial for durable and healthy pavement. These pipes are buried close to the foundation of the pavement construction for efficient water drainage [2]. In aquifer dewatering applications, Stuyt et al. [3] indicated that the inflow per unit length of a perforated pipe could not be

Corresponding author: ceremy@usm.my

constant. If native soils are permeable, Abida & Sabourin [4] discovered that a perforated pipe-grass swale design might substantially minimize storm runoff. Several researchers referred to a porous pipe as an orifice [5]. However, experimental findings reported in support of the orifice hypothesis have limitations due to the restricted number and range of variables investigated [6].

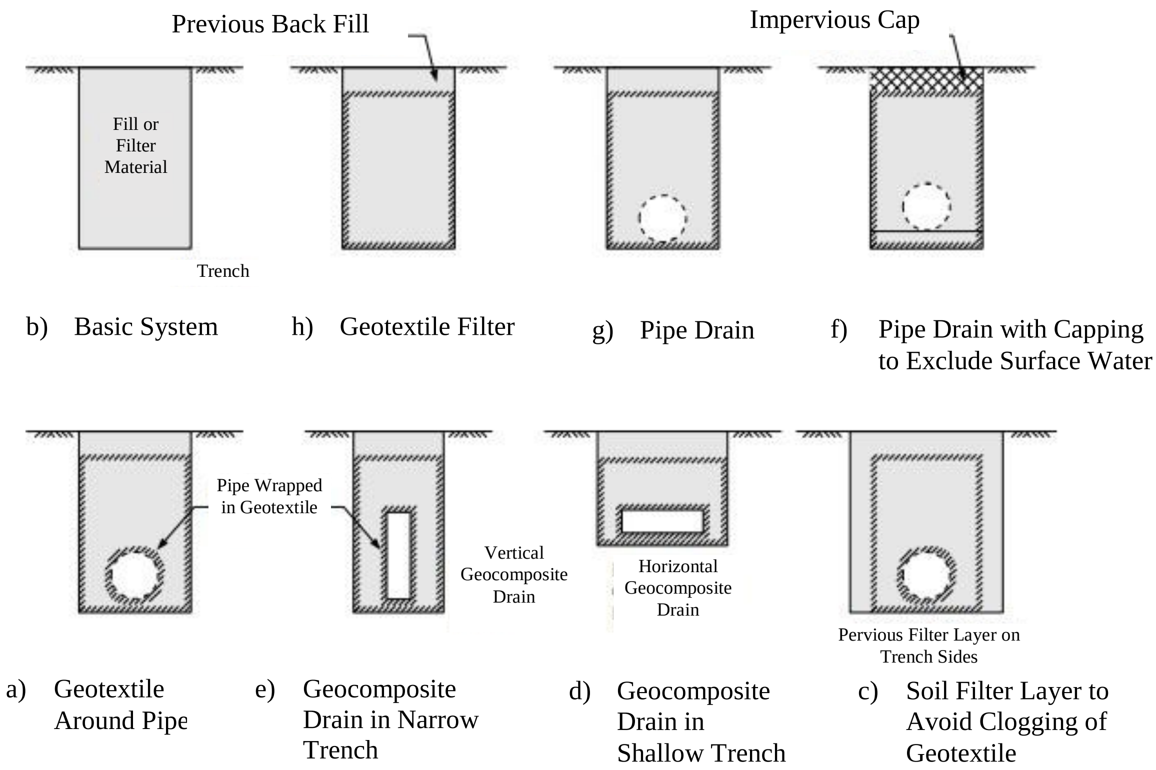

Fig. 1 - Types of subsoil drains [1]

A perforated subsurface drain (Fig. 2) is installed to intercept, collect, and transport surplus ground water to a stable outlet. It is often utilized for drainage purposes. Perforated subsurface drains are produced using a combination of high-frequency vibration and extrusion, which yields a durable pipe of excellent and consistent quality that is widely used for subsoil drainage to satisfy a variety of purposes. Unique to perforated subsurface drainage pipes is the fact that water infiltration occurs across the entire surface. The aim of this study is to determine the flow characteristics in perforated subsurface drain of drainage system application.

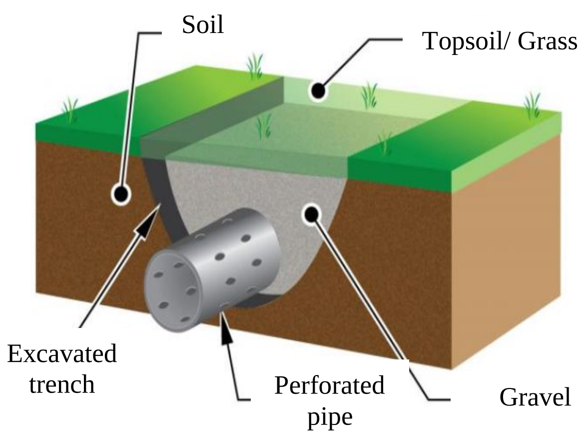

Fig. 2 - Perforated subsurface drain [7]

2. Methodology

This section describes the experimental process briefly. The experiment was conducted in a rectangular straight flume of 5.9m length at Physical Laboratory, River Engineering and Urban Drainage Research Centre (REDAC), Universiti Sains Malaysia. Fig. 3 illustrates a sectional sketch of an experimental channel. This channel's slope can be varied by adjusting using the adjusting jack. The experiment was conducted with a longitudinal slope of 1/500.

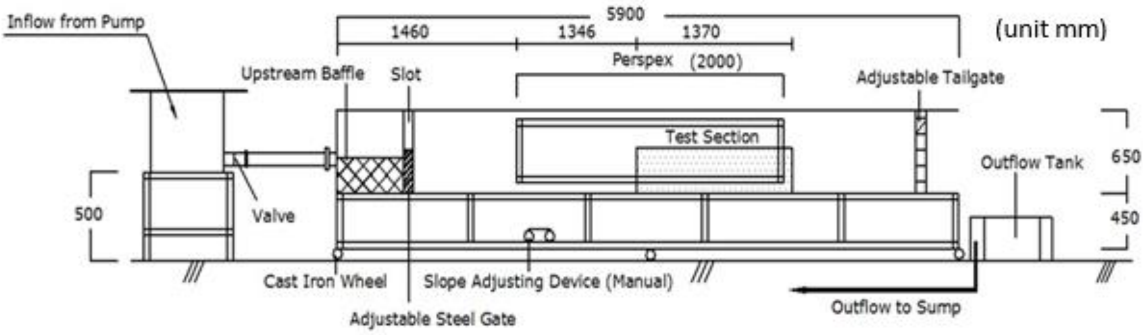

Fig. 3 - Sectional drawing of experimental channel [8]

As illustrated in Fig. 4, this laboratory test was set up with a single arrangement of corrugated High- Density Polyethylene (HDPE) with a standard diameter of 300 mm. As indicated in Fig. 5, a corrugated pipe wall with a smooth inner liner was selected for this study. In this investigation, nine segments were analyses. During the experiment, the depth and velocity of the flow were measured. Three measurements were averaged for each measurement to determine the average velocity and depth. The velocity is measured at $0.6Y$, which is (Y = flow depth). All measurements were performed with a consistent flow. 10 to 20 minutes are required for this experiment to steady the flow. Fig. 5 represents the flow in smooth inner perforated pipe.

Fig. 4 - The experiment set up

Fig. 5 - The perforated subsurface drain with smooth inner wall

2.1 Hydraulic Parameters

The Hydraulic parameters considered in this study are Froude Number (*Fr*), Reynolds Number (*Re*), flow depth (*y*), flow velocity, and discharge (*Q*). The analysis of the laboratory results was based on the Manning Formula was calculated from [5]:

$$n = \frac{1}{v} R^{\frac{2}{3}} S^{\frac{1}{2}} \tag{1}$$

where n = Mannings, v = Velocity (m/s), R = Hydraulic Radius and S = Slope. Froude number relates to the state of flow and is described in Table 1 [9].

$$Fr = \frac{V}{\sqrt{gY}} \tag{2}$$

where Fr =Froude number, V = the velocity of flow in m/s, g = acceleration of gravity in m^2/s, Y = the depth of the flow section in *m*.

Table 1 - State of flow described by Froude Number

Froude Number *Fr*	State of Flow	Description
$Fr = 1$	Critical	Flow celerity equal to flow velocity
$Fr < 1$	Subcritical	Slow flow-tranquil and streaming
$Fr > 1$	Supercritical	High velocity-rapid, shooting and torrential

The performance of manning was calculated by using the determination of R^2 [9].

$$R^2 = \left[\sum_{i=1}^{n} (O_i - \bar{O})(P_i - \bar{P}) \Big/ \sqrt{\sum_{i=1}^{n} (O_i - \bar{O})^2 \sum_{i=1}^{n} (P_i - \bar{P})^2} \right]^2 \tag{3}$$

3. Results and Discussion

This section presents the experimental results and discussion. Fig. 6 illustrates the relationship between manning and depth. The trend has been observed to be directly proportionate. The calculated range of manning is 0.008-0.011, while the calculated range of Reynolds number, *Re*, is 85085.17- 115737.39. The correlation value, *r* value, is 0.958, which is a positive addition (near to 1), and the *p*- value is calculated to be 0.000, which is statistically significant ($p < 0.05$). There is a correlation between the highest depth as well as the highest value of manning, *n*.

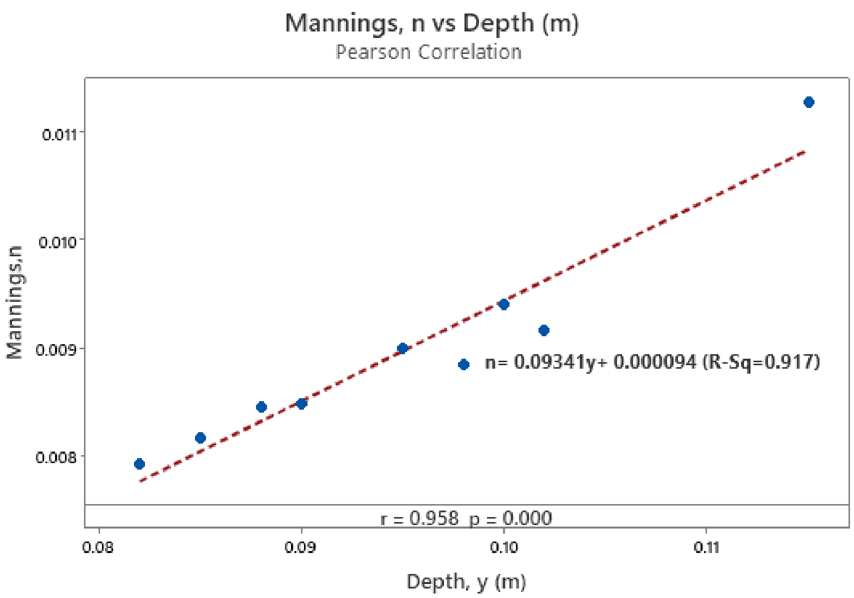

Fig. 6 - The relationship between Manning, n and depth (m)

Fig. 7 shows the relationship of manning, *n*, with velocity *(m/s)*. It was observed that the trend is directly inversely proportional. The standard manning's value of Polyethylene *PE* Corrugated with smooth inner walls the range of 0.009 - 0.015[4]. However, the value of manning for this study was calculated to be 0.008-0.011. The range of Reynolds number, *Re*, is calculated to be 85085.17-115737.39 (R^2=0.977). From the graph, it can be seen that the correlation value, *r* value is 0.996, which is a good agreement (close to 1), and the *p*-value is analyses to be 0.000, which is significant *(p* < 0.05). It can be related that the lowest velocity gives the higher value of the manning, *n*.

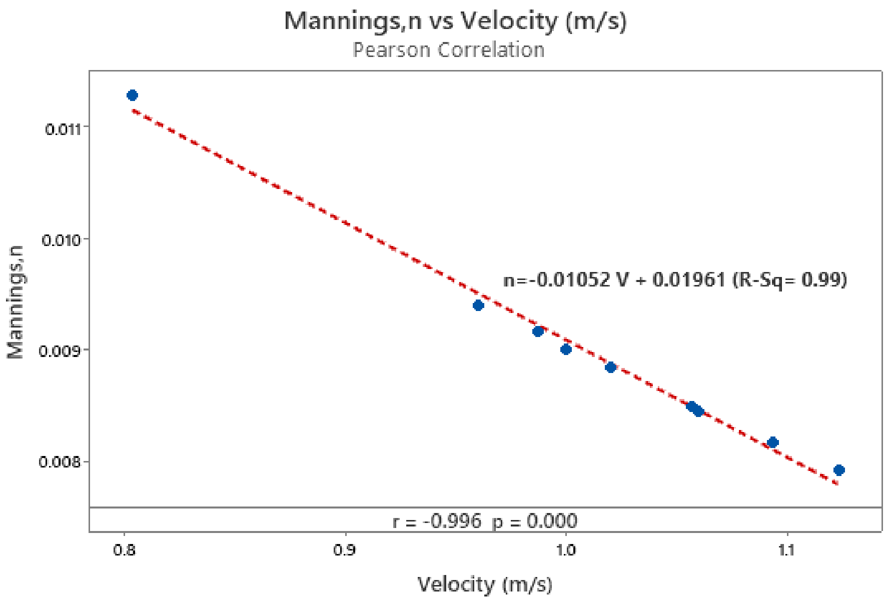

Fig. 7 - The relationship between Manning, *n* and velocity (m/s)

Fig. 8 shows the distribution of the manning, *n* and discharge (m^3/s). It can be seen that the distribution pattern is inversely proportional. It can be seen that the *r*-value was recorded to be - 0.973, which gives good agreement that the value close to 1. Moreover, the *p*-value is recorded to be 0.000, which is <0.05, which can be considered significant. The relationship between manning, *n* and discharge is n = -0.3181Q + 0.02697.

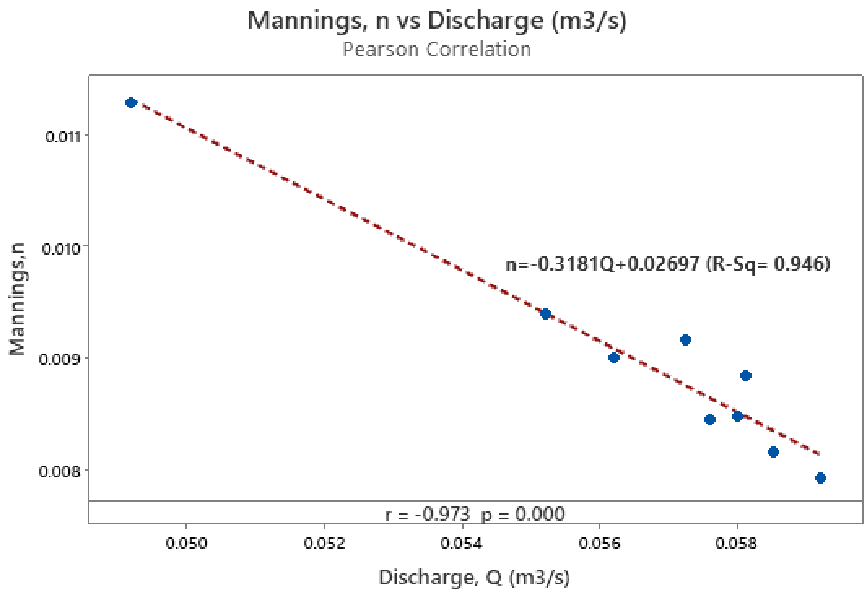

Fig. 8 - The relationship between manning, *n* and discharge (m^3/s)

A similar pattern was observed for manning *n* with Froude Number *(Fr)* as shown in Fig. 9. It can be seen that the trend is inversely proportional for manning, *n* and Froude number, *Fr*. The range of manning was recorded to be 0.008-0.011, and the value of the Froud Number was calculated to be 0.756-1.252. The sub-critical and supercritical flow occurred in this study. The *r*-value is observed to be -0.977 (closed to 1).

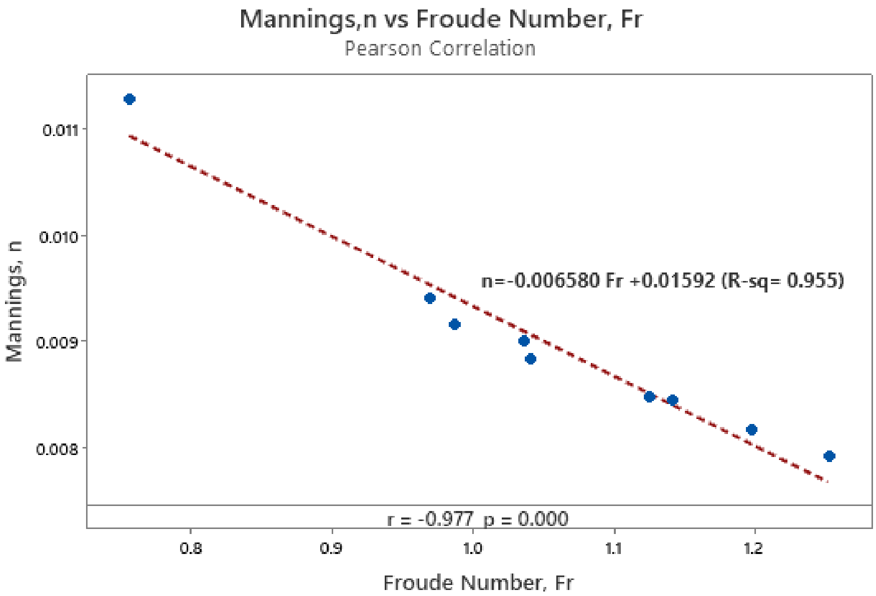

Fig. 9 - The relationship between manning, *n* and Froude Number

In order to verify the experiment, the results in terms of depth, velocity, discharge and manning from Muhammad et al. [9] is compared. The range of data collection from the previous study is shown in Table 1. The depth of water level of Muhammad et al. [9] is lower (0.04-0.08) from present study (0.08-0.12). Similar with other parameters of Muhammad et al. [9] the velocity and discharge give lowest value compared to present study. The presents study shows the calculated manning n are in the range 0.008-0.011 which is lower than (0.027-0.121) previous study Muhammad et al. [9]. At overall, this verify that the present study is good agreement in term of capacity discharge of water compared to Muhammad et al. [9]. The summary of all the relationships of manning, *n* and hydraulic parameters is shown in Table 2.

Table 2 - Range of data collected from previous study Muhammad et al. (2018) [9]

Parameter	Range
Depth, *Y* (m)	0.04-0.08
Velocity, *V* (m^2)	0.024-0.370
Discharge, *Q* (m^3/s)	0.005-0.061
Manning's Coefficient, *n*	0.027-0.121

4. Conclusion

The research was carried out to investigate flow resistance along the perforated subsurface drain. The condition of a gate fully open with a longitudinal slope of 1/500 is considered in this study to analyses the free flow without a gate opening. The results show the relationship between manning, *n* and another hydraulic parameter; for example, depth, velocity, discharge, and Froude number are significant, p-value < 0.05, and the r value is close to 1 in all cases. The sub-critical and supercritical, and turbulence flow has occurred in this study. At overall, this verify that the present study is good agreement in term of capacity discharge of water compared to Muhammad et al. [9]. In order to fully appreciate the effect of flow resistance along the perforated subsurface drain, other types of subsurface channels are recommended.

Acknowledgement

The authors express their gratitude to Universiti Sains Malaysia for the financial support of the Short- Term Grant (STG) (304/PREDAC/6315532) and for providing the facilities. This research is supported in part by the Ministry of Higher Education, Malaysia, under the Higher Institution Centre of Excellence (HICoE) for a research grant of 311.PREDAC.4403901.

References

[1] Department of Irrigation Malaysia (2020). Urban Stormwater Management Manual for Malaysia (MSMA).

[2] Afrin T., Khan A. A., Kaye N. B. & Testik F. Y. (2016) Numerical model for the hydraulic performance of perforated pipe underdrains surrounded by loose aggregate. Journal of Hydraulic Engineering, 142(8), 04016018.

[3] Stuyt L. C. P. M., Dierickx W. & Martinez Beltran J. (2005). Materials for subsurface land drainage systems. Food and Agriculture Organization of the United Nations, Rome.

[4] Abida H. & Sabourin J. F. (2006). Grass swale-perforated pipe system for stormwater management. Journal of Irrigation and Drainage Engineering. https://doi.org/10.1061/(ASCE)0733-9437(2006)132:1(55)

[5] Schwartz S. S. (2010). Effective curve number and hydrologic design of pervious concrete storm- water systems. Journal of Hydrologic Engineering, 15(6), 465-474.

[6] Murphy P., Kaye N. B. & Khan A. A. (2014). Hydraulic performance of aggregate beds with perforated pipe underdrains running full. Journal Irrigation and Drainage Engineering. https://doi.org/10.1061/(ASCE)IR.1943-4774.0000740

[7] Jarrod R. (2018). French drain design and cost, including pipe, gravel and installation. Engineeringclicks. https://www.engineeringclicks.com/french-drain/

[8] Kee L. C., Zakaria. N. A., Lau T. L., Chang C. K. & Ab Ghani A. (2011). Determination of Manning's n for subsurface modular channel. The 3rd International Conference on Managing Rivers in the 21st Century: Sustainable Solution for Global Crisis of Flooding, Pollution and Water Scarcity, pp. 1-8.

[9] Muhammad M. M., Wan Yusof K., Mustafa M., Zakaria. N. A. & Ab Ghani A. (2018). Hydraulic performance of subsurface drainage module. The 37th IAHR World Congress, Kuala Lumpur.

[10] Zainalfikry M. K., Ab Ghani A., Zakaria N. A. & Chan N. W (2020). Flow Resistance in Ecological Subdrainage Channel. AWAM International Conference on Civil Engineering. 10.1007/978-3-030-32816-0_84